Estimation of the electron temperature and density in the plasma of a Hall thruster

IEPC-2011-337

Presented at the 32nd International Electric Propulsion Conference,
Wiesbaden • Germany
September 11 – 15, 2011

J. Cavalier[1], N. Lemoine[2] and G. Bonhomme[3]
Institut Jean Lamour, UHP, 54506, Vandœuvre les Nancy, France

S. Tsikata[4], C. Honoré[5], D. Grésillon[6]
Laboratoire de Physique des Plasmas, Ecole Polytechnique, route de Saclay, 91128 Palaiseau, France

Abstract: The 3D dispersion equation of an instability observed at the exit of a Hall thruster plasma is studied. The equation is solved numerically in the warm and cold ion cases. A parametric study of its slope shows that the mode has a group velocity close to the speed of sound. Thus, the electron temperature is estimated using collective light scattering measurements to be 29 eV. On the other hand, an analytical model is developed to fit the experimental dispersion relation. This model agrees well with the numerical results and allows an estimation of both the electron temperature and density. For the first time at the exit plane of a Hall thruster, the electron temperature and density are estimated by a non-disturbing method.

Nomenclature

CLS	=	Collective Light Scattering
LIF	=	Laser Induced Fluorescence
NRMSE	=	Normalized Root Mean Square Error
x	=	direction of the electric field
y	=	opposite direction of the drift velocity
z	=	direction of the magnetic field
$\vec{k}$, k	=	observation wave vector, number [rad.m^{-1}]
k_x ,k_y, k_z	=	wave number in the x, y, z, direction [rad.m^{-1}]
f, ω	=	wave frequency, angular frequency [Hz, rad.s^{-1}]
T_i, T_e	=	ion, electron temperature [eV]
M_i, m_e	=	ion, electron mass [kg]
$\hat{M}$	=	ratio of the ion mass over electron mass [normalized]
n_e	=	electron density [m^{-3}]
E_0	=	constant electric field [V.m^{-1}]
B_0	=	constant magnetic field [T]
q	=	elementary charge [C]

[1] PhD student, jordan.cavalier@ijl.nancy-universite.fr
[2] Doctor, nicolas.lemoine@ijl.nancy-universite.fr
[3] Professor, gerard.bonhomme@ijl.nancy-universite.fr
[4] Doctor, sedina.tsikata@polytechnique.edu
[5] Research Engineer, cyrille.honore@polytechnique.edu
[6] Professor Emeritus, gresillon.dominique@wanadoo.fr

γ = adiabatic index [normalized]
λ_{Di}, λ_D = ion, electron Debye length [m]
ω_{ce} = electron cyclotron angular frequency [rad.s^{-1}]
ω_{pi} = ion plasma angular frequency [rad.s^{-1}]
V_d = drift velocity [m.s^{-1}]
v_{thi}, v_{the} = ion, electron thermal velocity [m.s^{-1}]
v_p = beam velocity [m.s^{-1}]
c_s = sound speed [m.s^{-1}]
v_g = group velocity [m.s^{-1}]
$\hat{\omega}, \hat{l}, \hat{v}$ = normalized angular frequency, length and velocity to, respectively, ω_{pi}, λ_D, c_s [normalized]
α = angle between the x-axis and the y-axis, 90° being in the y-direction [degree]
g = Gordeev function
Z, Z' = plasma dispersion function and its derivative
$InvZ'$ = inverse function of Z'
I_m = modified Bessel function of first kind of order m

I. Introduction

An instability known as the beam-cyclotron instability[1] leads to the growth of a longitudinal wave. This occurs when a beam is incident on a magnetized plasma in a direction orthogonal to the magnetic field. Similarly, such an instability can be found in Hall thrusters[2-4], where the electrons drift azimuthally due to an axial electric field and a crossed radial magnetic field. A study of the 2D dispersion relation (wave vector orthogonal to the magnetic field, k_z null) has shown a mode which exists only for a discrete number of wave vectors[5]. However, recent measurements by Collective Light Scattering[6] (CLS) have pointed out that the wave vector has a component along the magnetic field direction (k_z) and that the associated dispersion relation is continuous. Accordingly, we propose here to study the dispersion relation in the 3D case.

In Section II, the theoretical 3D dispersion relation is presented. The cold ions hypothesis is then considered based on Laser Induced Fluorescence (LIF) measurements[7]. Section III is devoted to the numerical solving of this equation. The typical values of the parameters are also set up. In Section IV, the slope of the numerical dispersion relation is studied. As it is found to be proportional to the speed of sound, the electron temperature can be estimated from CLS measurements. Based on the evanescent magnetic field limit, an analytical model is developed in Section V allowing to measure both the temperature and density of electrons. First, the model is shown to be in good agreement with the numerical dispersion relation. Second, an experimental dispersion relation is fitted and the electron temperature and density are estimated.

II. The dispersion relation

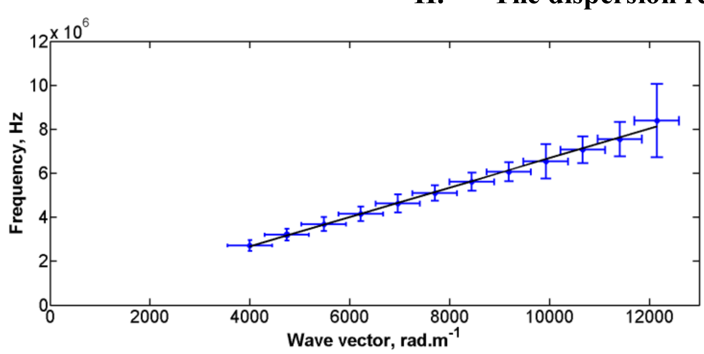

Figure 1. Dispersion relation observed by collective light scattering in the y-direction.
Blue dots: experimental data, black line: linear fit.

A dispersion relation observed by CLS looking in the y-direction is shown in Fig. 1. The frequency is found to depend quite linearly and continuously on the wave vector, leading to a group velocity of v_g = 4210 m.s^{-1}, being close to the expected speed of sound c_s. The intercept of the linear fit is close to zero (17.9 kHz) and thus, the wave seems similar to an ion acoustic wave, with a dispersion relation which can be written as $\omega = v_g \times k$. However, the ion acoustic mode in fluid theory propagates parallel to the magnetic field[8] while the mode observed by CLS propagates orthogonally to it. In order to clarify this point, the 3D dispersion relation is written using kinetic theory.

A. Warm ion case

The plasma at the exit of a Hall thruster may be approximated as a collisionless plasma[9], subject to an uniform magnetic field $\vec{B}_0$ parallel to the z-axis and an uniform electric field $\vec{E}_0$ parallel to the x-axis, in a slab geometry. The electrons are magnetized while the ions are not. The drift velocity $\vec{V}_d = \frac{\vec{E}_0 \times \vec{B}_0}{B_0}$ is parallel and opposite to the y-axis. In the case of a Maxwellian distribution for both ions and electrons, the kinetic theory leads to:

$$1+\frac{1}{k^2\lambda_D^2}\left[1+g\left(\omega,k,V_d,v_{the},\omega_{ce}\right)\right]-\frac{1}{2k^2\lambda_{Di}^2}Z'\left(\frac{\omega-k_x v_p}{\sqrt{2}kv_{thi}}\right)=0 \tag{1}$$

where $g\left(\omega,k,V_d,v_{the},\omega_{ce}\right)$ is the Gordeev function[10]:

$$g\left(\omega,k,V_d,v_{the},\omega_{ce}\right)=\frac{\omega-k_y V_d}{k_z v_{the}\sqrt{2}}e^{-\left(\frac{k_\perp v_{the}}{\omega_{ce}}\right)^2}\sum_{m=-\infty}^{+\infty}Z\left(\frac{\omega-k_y V_d-m\omega_{ce}}{k_z v_{the}\sqrt{2}}\right)I_m\left(\left(\frac{k_\perp v_{the}}{\omega_{ce}}\right)^2\right) \tag{2}$$

Equation (1) is the so called 3D dispersion relation which must be solved in ω. The angular frequency ω depends on many parameters (k_x, k_y, k_z, λ_D, V_d, v_{the}, v_{thi}, v_p, ω_{ce}) and is not easily found. However, Eq. (1) can be simplified using LIF measurements and the number of parameters are reduced by one.

B. Cold ions case

In the y-direction, the ion temperature is believed to be small compare to that of electrons[7]. Thus, $T_i \to 0$ and Z' reduces to:

$$Z'\left(\frac{\omega-k_x v_p}{\sqrt{2}k v_{thi}}\right)\underset{T_i\to 0}{\rightarrow}\frac{2v_{thi}^2 k^2}{\left(\omega-k_x v_p\right)^2} \tag{3}$$

Accordingly, Eq. (1) becomes

$$\left(\omega-k_x v_p\right)^2=\frac{k^2\lambda_D^2\omega_{pi}^2}{1+k^2\lambda_D^2+g\left(\omega,k,V_d,v_{the},\omega_{ce}\right)} \tag{4}$$

From Eq. (4), it is clear that the two parameters ω_{pi} and λ_D can be used to normalize, respectively, the angular frequency and the length. Consequently, the velocities are normalized by $c_s=\lambda_D\,\omega_{pi}$. Thus, Eq. (4) leads to:

$$\left(\hat{\omega}-\hat{k}_x\hat{v}_p\right)^2=\frac{\hat{k}^2}{1+\hat{k}^2+g\left(\hat{\omega},\hat{k},\hat{V}_d,\hat{\omega}_{ce},\hat{M}\right)} \tag{5}$$

and Eq. (2) becomes:

$$g\left(\hat{\omega},\hat{k},\hat{V}_d,\hat{\omega}_{ce},\hat{M}\right)=\frac{\hat{\omega}-\hat{k}_y\hat{V}_d}{\hat{k}_z\sqrt{2\hat{M}}}e^{-\hat{M}\left(\frac{\hat{k}_\perp}{\hat{\omega}_{ce}}\right)^2}\sum_{m=-\infty}^{+\infty}Z\left(\frac{\hat{\omega}-\hat{k}_y\hat{V}_d-m\hat{\omega}_{ce}}{\hat{k}_z\sqrt{2\hat{M}}}\right)I_m\left(\hat{M}\left(\frac{\hat{k}_\perp}{\hat{\omega}_{ce}}\right)^2\right) \tag{6}$$

It is worth mentioning that the normalized angular frequency depends on the three normalized parameters: $\hat{v}_p, \hat{V}_d$, $\hat{\omega}_{ce}$. In the next Section, Eqs. (1) and (4) will be numerically solved and the influence of the different parameters on ω will be studied.

III. Numerical solving

A. Order of magnitude

Equations (1) and (4) have to be solved analytically. An iterative scheme can be found looking carefully at the order of magnitude of the different terms. Especially, the expression of the Gordeev function (Eq. (2)) can be simplified using results from CLS. In fact, the angular frequency was found to be of the order of ω=6.10^7 rad.s^{-1} at maximum for a corresponding wave vector of k_y=12000 rad.m^{-1}. On the other hand in the Snecma X000 Hall-effect thruster case, V_d and ω_{ce} are estimated to be of the order of 7.10^5 m.s^{-1} and 3.10^9 rad.s^{-1}, respectively leading to $k_yV_d \gg \omega$ and $|k_yV_d+m\,\omega_{ce}| \gg \omega$ for m and k_y having the same sign. Whereas for m and k_y having an opposite sign, there is some ambiguity depending on the exact value of k_y, V_d and ω_{ce}, yet the approximation is still considered.

Thus, it is possible to calculate the angular frequency from Eqs. (1) and (4) by iteration. As a first step, ω is set to zero in the Eq. (2) and Eqs. (1) and (4) become, respectively:

$$\omega_1 = k_x v_p + \sqrt{2} v_{thi} k \, InvZ' \left\{ 2k^2 \lambda_{Di}^2 + 2\hat{T}\left[1 + g\left(k, V_d, v_{the}, \omega_{ce}\right)\right]\right\} \quad (7)$$

and

$$\left(\omega_1 - k_x v_p\right)^2 = \frac{k^2 \lambda_D^2 \omega_{pi}^2}{1 + k^2 \lambda_D^2 + g\left(k, V_d, v_{the}, \omega_{ce}\right)} \quad (8)$$

where the index $_1$ stands for the first iteration.

The inverse Z' function ($InvZ'$) can be found using a method which is not described here. When calculating numerically, ω_1 is reintroduced in Eq. (2) to recalculate the Gordeev function. Then ω_2 is calculated using, respectively for the warm and cold case:

$$\omega_2 = k_x v_p + \sqrt{2} v_{thi} k \, InvZ' \left\{ 2k^2 \lambda_{Di}^2 + 2\hat{T}\left[1 + g\left(\omega_1, k, V_d, v_{the}, \omega_{ce}\right)\right]\right\} \quad (9)$$

and

$$\left(\omega_2 - k_x v_p\right)^2 = \frac{k^2 \lambda_D^2 \omega_{pi}^2}{1 + k^2 \lambda_D^2 + g\left(\omega_1, k, V_d, v_{the}, \omega_{ce}\right)} \quad (10)$$

where the index $_2$ stands for the second iteration.

This process is repeated until the error is low enough. The errors are determined by injecting ω in Eqs. (1) and (4), respectively. Now that the two equations can be solved numerically, some typical parameters for the plasma of a Snecma X000 Hall-effect thruster will be introduced.

B. Usual parameter's values

Table 1. Typical values[11] of the Snecma X000 Hall-effect thruster

m_e (kg)	M_i (kg)	E_0 (V.m^{-1})	B_0 (T)	n_e (m^{-3})	T_e (eV)	λ_D (m)	ω_{pi} (rad.s^{-1})	c_s (m.s^{-1})
9.11×10^{-31}	2.2×10^{-25}	10^4	15×10^{-3}	10^{18}	15	3×10^{-5}	1.2×10^8	3433

For reference, the thruster and plasma parameters at the exit of the Snecma X000 Hall-effect thruster are summarized in Table 1. The three parameters λ_D, ω_{pi}, c_s used for the normalization are also given. The two values for electron temperature and density are rough estimations from numeric codes.

Table 2. Typical values of normalized parameters.

$\hat{k}_x$	$\hat{k}_y$	$\hat{k}_z$	$\hat{M}$	$\hat{v}_p$	$\hat{V}_d$	$\hat{\omega}_{ce}$
0	0.01-1	0.03	2.4×10^5	0	200	25

In this part, the normalized Eqs. (5) and (6) are considered. A set of typical values for the different normalized parameters is given in Table 2. As the mode is seen in the y-direction, it is common to choose $\hat{k}_y$ as the variable and it lies between 0.01 and 1 (corresponding to 300 and 30000 rad.m^{-1}). The mode is seen perpendicularly to the electric field, thus, $\hat{k}_x$ can be set as null. In previous studies, the 2D dispersion relation was considered[5], $\hat{k}_z$ being null. However, CLS measurements have shown that this parameter is non-vanishing. In Fig. 2, the influence of $\hat{k}_z$ on the normalized angular frequency $\hat{\omega}$ is presented, other parameters being set as in Table 2. As expected,

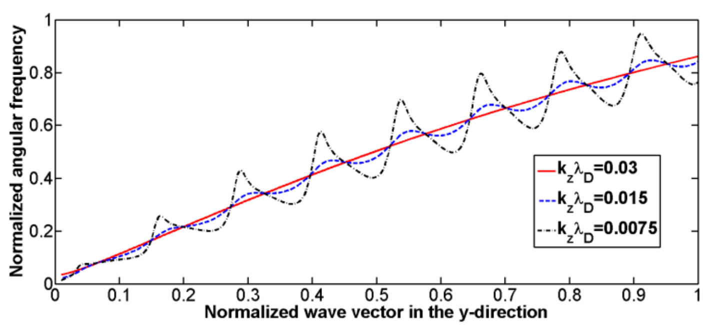

Figure 2. Angular frequency as a function of $\hat{k}_y$ for different $\hat{k}_z$.

Full, dashed and dash-dotted lines correspond respectively to $\hat{k}_z$=0.03, 0.0015, 0.0075.

resonances are observable for low values of $\hat{k}_z$ while for higher values, the curve is smoothed. In experiment, a quite linear and smooth curve was observed, as shown by Fig. 1. Consequently, $\hat{k}_z$ is set as 0.03 (corresponding to 1000 rad.m^{-1}) for which no resonances are observed on the curve.

As it can be seen from Eq. (5), the beam velocity $\hat{v}_p$ only affects the angular frequency as a Doppler effect and can be omitted, looking in the y-direction. $\hat{V}_d$ and $\hat{\omega}_{ce}$ can lie in between 50-300 and 5-65 respectively. The ratio of masses $\hat{M}$ is equal to 2.4×10^5 for Xenon gas. The main parameters being set up, the theoretical dispersion relation can be studied. Due to the linearity of the experimental dispersion, a parametric study of the numerical slope will be made as a first attempt to estimate the electron temperature.

IV. Slope of the dispersion relation

A. Dependence of the slope with $\hat{\mathbf{V}}_d$ and $\hat{\boldsymbol{\omega}}_{ce}$

CLS measurements indicate a linear dependence of ω with k leading to a group velocity equal to 4210 m.s^{-1}, as shown in Fig. 1. Consequently, the slope of Eq. (5) is studied for different values of the parameters. This slope is obtained by linearly fitting the equation between $\hat{k}_y$=0.05 and 0.4, which is the expected interval of CLS measurements. Figure 3 shows the evolution of this slope with $\hat{V}_d$ and $\hat{\omega}_{ce}$, other parameters being set as in Table 2. It is clear from Fig. 3 that for $\hat{\omega}_{ce}$ less than 35, the normalized slope hardly depends on the two parameters and is equal to 0.9. However, as the dispersion relation is less linear when $\hat{\omega}_{ce}$ increases to higher values than 35, the normalized slope is seen to differ from 0.9. Because of the linearity of the experimental dispersion relation, values higher than 35 are eliminated. Accordingly, the slope is found to be almost constant with $\hat{V}_d$ and $\hat{\omega}_{ce}$.

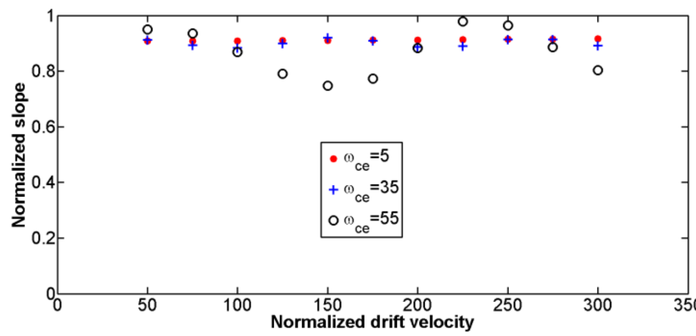

Figure 3. Normalized slope as a function of the normalized drift velocity for different normalized electron cyclotron frequency.
Dots, crosses and open circles correspond respectively to $\hat{\omega}_{ce}$=5, 35, 55.

B. Estimation of $\mathbf{T_e}$ with the slope

Therefore, the slope of the mode can be equaled to $0.9\times c_s$. Using the experimental slope (4210 m.s^{-1}) and the Xenon mass (2.175×10^{-25} kg), T_e is estimated to be 29 eV. The experiment was performed with a flow rate of 18 mg.s^{-1} and an apply voltage of 300 V.

In recent CLS measurements (obtained for different operation parameters than Fig. 1), a curvature of the dispersion relation was observed. This new observation would allow determining two plasma parameters instead of only one with a straight curve. Thus, the electron density could be estimated in addition of the electron temperature. However, to do that, it is necessary to develop an analytical model which depends on less parameters than Eq. (4).

V. Analytical model

A. Evanescent magnetic field

In this part, a new assumption is made in order to develop a model allowing to determine the electron temperature and density. As shown in Fig. 4 plotted for values set as in Table 2, decreasing $\hat{\omega}_{ce}$ reduces the resonances on the curve. No such resonances were observed by CLS and so, low magnetic field can be assumed.

In the limit of a zero magnetic field, it has been demonstrated[10] that the Gordeev function (see Eq. (6)) should be replaced by $\xi Z(\xi)$, where $\xi = -\frac{V_d}{v_{the}} = -\frac{\hat{V}_d}{\sqrt{\hat{M}}}$. The mandatory conditions are that $-\frac{\hat{k}\hat{V}_d}{\hat{\omega}_{ce}}$ and $\frac{\hat{k}\sqrt{\hat{M}}}{\hat{\omega}_{ce}}$ tend to infinity while ξ remains constant. These limits are not fully justified in the thruster case but allow developing a model which depends on the parameters T_e, n_e and V_d or only on $\hat{V}_d$ in the normalized case. Thus, Eq. (4) can be re-written as:

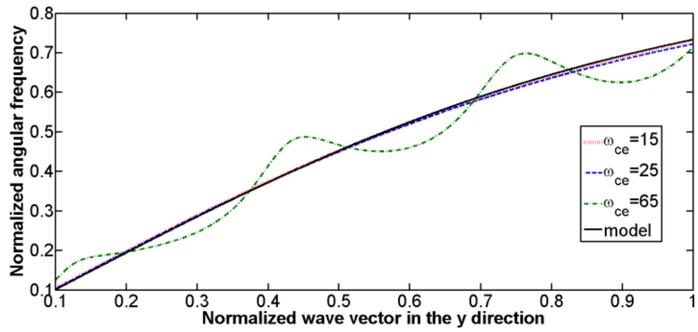

Figure 4. Normalized angular frequency as a function of $\hat{k}_y$ for different normalized electron cyclotron frequency.

Dotted, dashed and dash-dotted lines correspond to $\hat{\omega}_{ce}$=15, 25, 65, respectively. The full line corresponds to the model.

$$\omega^2 = \frac{k^2 \lambda_D^2 \omega_{pi}^2}{1 + k^2 \lambda_D^2 + \xi Z(\xi)} \tag{11}$$

or in normalized the case, Eq. (5) becomes:

$$\hat{\omega}^2 = \frac{\hat{k}^2}{1 + \hat{k}^2 + \xi Z(\xi)} \tag{12}$$

Before using the model on an experimental dispersion relation, it should be compared with the numerical solution.

B. Comparison of the model with the numerical solution

In this Section, Eq. (12) is used to fit the cold ions expression (Eq. (5)) through the parameter $\hat{V}_d$. The equation is fitted for values of $\hat{k}_y$ between 0.1 and 1.1. Then, $\hat{V}_d$ obtained from the fit is plotted versus the $\hat{V}_d$ input for different values of $\hat{\omega}_{ce}$, other parameters being set as in Table 2. The result is visible in Fig. 5. In a perfect case, the fitted value should be equal to the input value and should be on the first bisector. However, a slight difference is observable which is enhanced by increasing $\hat{V}_d$ input; and this is the case for all values of $\hat{\omega}_{ce}$. It is not yet understood why such a deviation from the ideal case is greater for $\hat{\omega}_{ce}$=5 while

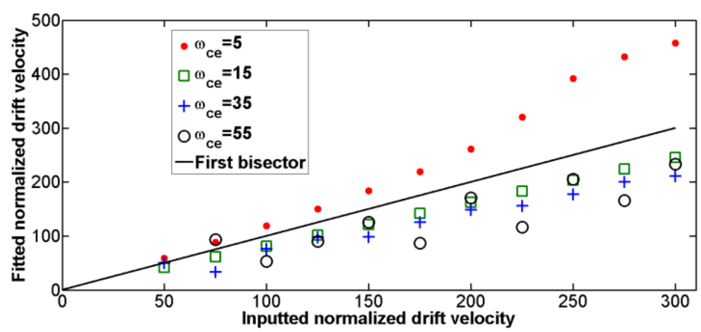

Figure 5. Fitted value versus inputted of the normalized drift velocity for different normalized electron cyclotron frequency.

Dots, open squares, crosses and open circles correspond to $\hat{\omega}_{ce}$=5, 15, 35, 55 respectively.

the model should agree more with the numerical solution for low values of $\hat{\omega}_{ce}$. Nevertheless, $\hat{\omega}_{ce}$ is believed to lie between 15-35 and $\hat{V}_d$ between 100-250 where the model fits quite well with the cold ions expression. Thus, the analytical expression (Eq. (11)) can be used to determine the electron temperature and density.

C. Estimation of the electron temperature and density

Now that the model has shown a good agreement with the numerical resolution, an experimental dispersion relation can be fitted to obtain some plasma parameters. As shown by Eq. (11), the model depends on three parameters: T_e, n_e and V_d.

V_d can be known from LIF measurements and is estimated to be 7.5×10^5 m.s^{-1}. Unfortunately, the curve in Fig. 1 is linear allowing to measure only one parameter. In fact, applying Eq. (11) to the experimental points leads to T_e=25.1±1.4 eV and n_e varying from $-\infty$ to $+\infty$ with a Normalized Root Mean Square Error (NRMSE) of 1.7×10^{-2}. The fit can be seen in Fig. 6. If the value obtained for T_e is in good agreement with that obtained by equaling the group velocity to $0.9\times c_s$, the linear dependence of the frequency prohibits determining n_e.

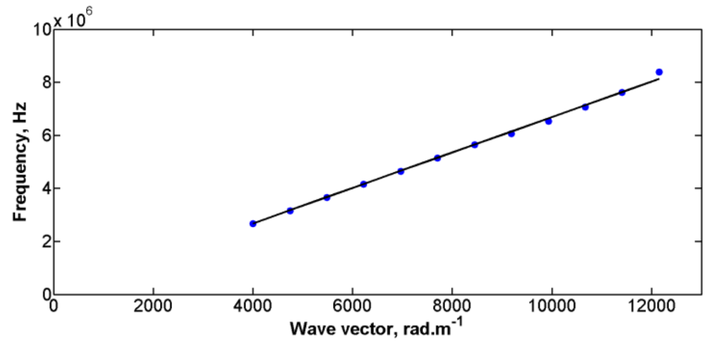

Figure 6. Dispersion equation fitted by the model.
The blue dots are the experimental points, the black line the fit by the model from Eq. (11) for V_d=7.5×10^5 m.s^{-1}.

However, in recent CLS measurements, a curvature of the dispersion relation was observed for different thruster parameters than in the case of Fig. 1. Unfortunately, for this experiment, the wave vector was not strictly in the y-direction (α=104°, 90° being in the y-direction) and had a small component in the x-direction shifting the frequency by Doppler effect. Nevertheless, it is possible to correct this effect by estimating the beam velocity v_p. An angular exploration around the y- and x-axis was realized by CLS to observe the evolution of the frequency with k_x and k_y. This α-exploration is visible in Fig. 7 and was realized rotating the wave vector in the (xy)-plan, keeping its norm constant. In the y-direction (α=90°), the angular frequency is a constant ω_0 which does not depend on α. Moving from the y-axis, the Doppler effect $\vec{k}\cdot\vec{v}_p$ must be taken into account, with $\vec{v}_p = v_p\vec{e}_x$ and $\vec{e}_x$ being the unitary vector in the $\vec{E}_0$ direction. Thus, the angular frequency in function of alpha can be written as:

$$\omega(\alpha)=\omega_0+k\cos(\alpha)v_p \tag{13}$$

Accordingly, a fit of the frequency around α=90° was realized using Eq. (13) and is shown in Fig. 7. The fit values are ω_0=2.3×10^7±8.3×10^5 rad.s^{-1} and v_p=2632±240 m.s^{-1} with a NRMSE of 4.6×10^{-2}. The beam velocity is much lower than expected for Hall thruster (a value of 2×10^4 m.s^{-1} was expected). In fact, the problem of localization of the observation volume is addressed for CLS. The root mean square observation length is of the order of 10 cm, being comparable to the thruster diameter (15 cm) and so the signal of the mode can come from the whole diameter. However, it has been shown[4] that the signal comes from the external periphery of the thruster. At this position, the coordinate of the beam velocity along the x-axis could be lower than at the center of the thruster and justify the low value found above.

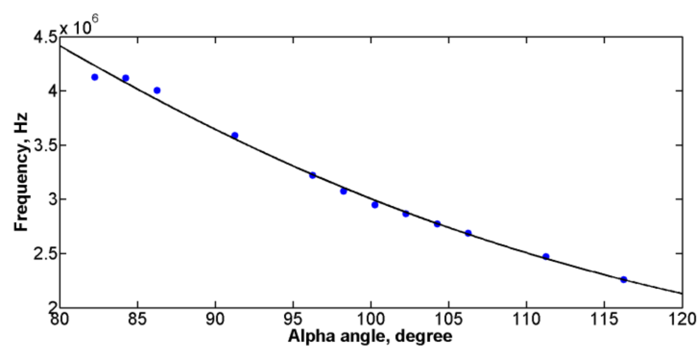

Figure 7. Frequency as a function of the angle between the electric field and the azimuthal direction for a wave vector equal to 8298.5 rad.m^{-1}.
Blue dots: experimental data, black line: fit $2\pi f$=ω_0+$k\cos(\alpha)v_p$.

Considering v_p=2632 m.s^{-1}, the frequency f observed at α=104° is corrected by adding the Doppler effect: $f_{cor}=f+101\times k$. The frequencies f_{cor} and f versus the wave vector k are plotted in Fig. 8. Once again, it is worth mentioning that the points from Fig. 8 and Fig. 1 were obtained for different thruster conditions, probably explaining the shape difference of the dispersion relation.

A fit of the corrected frequency is realized, using the analytical model (Eq. (11)) with V_d=7.5×10^5 m.s^{-1}. The parameters obtained are T_e=24.9±2.8 eV and n_e=1.2×10^{17}±1.9×10^{16} m^{-3} with a NRMSE of 3.7×10^{-2}. The corresponding curve is plotted in Fig. 8. T_e is found to be close to 25 eV, in good agreement with the value obtained with the slope in Section IV. The electron density has a lower value than in Table 1 but the two parameters are estimated at the external periphery of the thruster where values might be lower than at the center.

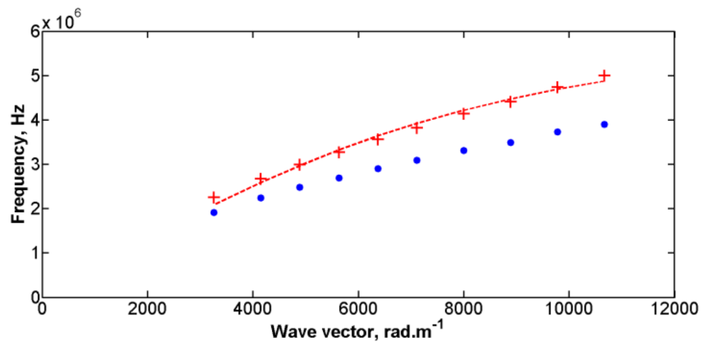

Figure 8. Frequency as a function of the wave vector. The blue dots are the experimental points obtained for an angle of 104°, the red crosses are the corrected points and the dashed line is the fit of the corrected point with the model from Eq. (11), for V_d=7.5×10^5 m.s^{-1}.

Using the values of T_e and n_e found above and k=8298.5 rad.m^{-1}, ω_0 can be recalculated with Eq. (11) and compared to the experimental value. ω_0 is calculated to be 2.7×10^7 rad.s^{-1} which is quite comparable to the experimental angular frequency ω_0=2.3×10^7. Thus, the estimation of T_e and n_e is in good agreement with the experimental observations.

Moreover, using these values, the model (Eq. (12)) can be used to fit the cold ions expression (Eq. (5)) through the parameter $\hat{V}_d$, as realized to obtain Fig. 5. The corresponding values of $\hat{V}_d$, $\hat{\omega}_{ce}$ and $\hat{k}_z$ are 155, 66 and 0.11, respectively. $\hat{k}_y$ lies in between 0.36 and 1.32, which is the corresponding range of CLS measurements. The fit gives a value for $\hat{V}_d$ of 128, not far 155.

VI. Conclusion

The studies of the 3D dispersion relation coupled with Collective Light Scattering (CLS) measurements have shown the possibility to estimate the electron temperature and density. The numerical slope of the dispersion relation has been identified to be close to the speed of sound. Using a slope obtained experimentally by CLS measurements, the electron temperature has been estimated to be 29 eV. On the other hand, a theoretical model has been developed to fit the dispersion relation. This model, depending on the electron temperature and density and the drift velocity, has shown to agree quite well with the theoretical dispersion equation. Accordingly, it has been used to fit the experimental frequency. For the first time at the exit plane of a Hall thruster, the electron temperature and density are estimated by a non-disturbing method.

Acknowledgements

The authors thank the CNES and SNECMA for their financial support. This work was performed in the frame of the joint-research program GdR 3161 between CNRS, CNES, Snecma and several Universities.

References

[1]Lampe, M., Manheimer, W. M., McBride, J. B., Orens, J. H., Shanny, R., Sudan, R. N., “Nonlinear Development of the Beam-Cyclotron Instability”, *Phys. Rev. Lett.*,Vol. 26, No. 20, 1971, pp. 1221, 1225.

[2]Tsikata, S, Lemoine, N., Pisarev, V. and, Grésillon, D. M., “Electron density fluctuations in a Hall thruster: observations by collective light scattering”, *J. Plasma Fusion Res. SERIES*, Vol. 8, 2009, pp. 1556, 1559.

[3]Tsikata, S, Lemoine, N., Pisarev, V. and, Grésillon, D. M., “Dispersion relations of electron density fluctuations in a Hall thruster plasma, observed by collective light scattering”, *Phys. Plasmas*, Vol. 16, 2009, pp. 033506, 033506(10).

[4]Tsikata, S, Honoré, C, Lemoine, N., and, Grésillon, D. M., “Three-dimensional structure of electron density fluctuations in the Hall thruster plasma: ExB mode”, *Phys. Plasmas*, Vol. 17, 2010, pp. 112110, 112110 (10).

[5]Ducrocq, A, Adam, J. C., Héron, A., and Laval, G., “High-frequency electron drift instability in the cross-field configuration of Hall thrusters”, *Phys. Plasmas*, Vol. 13, 2006, pp. 102111-102111(8).

[6]Tsikata, S, Honoré, C, Lemoine, N., and, Grésillon, D. M., "Collective light scattering for the study of fluctuations in magnetized plasmas: the Hall thruster case study", *Contrib. Plasma Phys.*, Vol. 51, No. 2-3, 2011, pp. 119, 125.

[7]Bourgeois, G, Mazouffre, S., and Sadeghi, N., "Unexpected transverse velocity component of Xe^+ ions near the exit plane of a Hall thruster", *Phys. Plasmas*, Vol. 17, 2010, pp. 113502-113502(6).

[8]Bittencourt, J. A., *Fundamentals of Plasmas Physics*, 3rd ed., Springer-Verlag, New York, 2004, Chap. 17.

[9]Adam, J. C., Boeuf, J. P., Dubuit, N., Dudeck, M., Garrigues, L., Gresillon, D., Heron, et al., "Physics, simulation and diagnostics of Hall effect thrusters", *Plasma Phys. Control. Fusion*, Vol. 50, 2008, pp. 124041(17).

[10]Gordeev, G. V., JEPT (USSR), 6, 660 (1952).

[11]Tsikata, S.,"Small-Scale Electron Density Fluctuations in the Hall Thruster, Investigated by Collective Light Scattering", Ph.D. Dissertation, Laboratoire de Physique des Plasmas, Ecole Polytechnique., Palaiseau, France, 2009.

[12]Schmitt, J. P. M., "The magnetoplasma dispersion function: some mathematical properties", *J. Plasma Physics*, Vol. 12, 1974, pp. 51-59..